A Bias Controller for Si Mach-Zehnder Modulator

Hyun-Kyu Kim, *Graduate Student Member, IEEE*, Kihun Kim, Min-Hyeok Seong, *Graduate Student Member, IEEE*, Yongjin Ji, and Woo-Young Choi, *Member, IEEE*

***Abstract*— We demonstrate a controller that can automatically determine the on-chip heater voltage required for the quadrature bias of the Si photonic Mach-Zehnder Modulator (MZM) and maintain this condition against fluctuations in temperature or the input optical power. The controller is implemented with an FPGA together with monitoring and driving circuits. Its operation is successfully demonstrated with a fabricated Si single-drive push-pull MZM.**

***Index Terms*— Silicon photonics, Si Mach–Zehnder modulator, MZM bias controller.**

I. Introduction

IN RESPONSE to the explosive growth of cloud-based services and the consequential increase in demands for higher bandwidth interconnects, cost-effective optical connectivity solutions based on Si photonic integrated circuits (PIC) are getting a great amount of research and development attention. One of key devices for realizing high-performance Si PIC is the Mach-Zehnder Modulator (MZM), which is widely used in high-bandwidth data center transceivers [1]. In addition, Si MZMs are used for converting RF signals into the optical domain for microwave photonics applications [2], [3].

Since there is unavoidable uncertainty in the length difference between two arms of any Si MZM device due to the fabrication process variation, for any Si MZM application, a calibration process is required in which the length difference is controlled with an on-chip heater so that the optimal bias condition can be achieved. Furthermore, this condition should be maintained against any environmental fluctuation. For these, various MZM control techniques have been reported [4], [5], [6], [7]. The harmonic monitoring method with a low-frequency pilot tone can be used, where the optimal bias condition is achieved by monitoring the fundamental and the second-order terms of the pilot tone [4], [5]. However, using a pilot tone requires low-pass filters for filtering out the pilot tone from the signal and this may require the large chip area especially if these filters are realized with the IC technology. To overcome this problem, a direct monitoring method of $LiNbO_3$ MZM [6] has been reported in which the optical modulation amplitude (OMA) of the modulated signal is monitored and maximized. This method has the advantage of direct MZM OMA monitoring, but it can consume a lot of power because it has to process high-frequency signals especially in high data-rate applications. In [7], authors present a $LiNbO_3$ MZM control method based on coherent detection, which enables various modulation format. However, this method required additional optical components as well as complex post data processing. In addition, direct bias voltage control as is done for $LiNbO_3$ MZM cannot be applied to Si MZMs. This is because the amount of the refractive index change provided by the PN junction bias voltage change is very small and non-linear and it is very difficult to bring the device to the desired transmission point with the bias voltage change alone. For this reason, the optimal transmission point of the Si MZM is achieved with on-chip heaters.

In this letter, we demonstrate an FPGA-based controller with which the quadrature bias condition of a Si MZM is automatically determined in the calibration step (scan mode) and maintained during the Si MZM operation (lock mode). During the scan mode, the controller scans the on-chip heater driving voltages and measure the corresponding MZM transmission characteristics, from which the quadrature bias condition is determined. During the lock mode, the quadrature bias condition is maintained by dithering the heater voltage and changing the heater bias voltage if the monitored transmission characteristics are not optimal. Although the controller is implemented with an FPGA, the implemented control hardware is simple enough so that it can be easily realized with a custom-designed IC, which can greatly reduce the size and the power consumption of the controller.

This letter is organized as follows. In Section II, the control scheme is explained. In Section III, measurement results are presented, which demonstrate the effectiveness of our control scheme. Finally, the letter is concluded in Section IV.

II. Bias Control Scheme for Silicon Mach-Zehnder Modulator

Figure 1 shows the structure of a Si MZM. It has two multi-mode interferometers (MMIs): one 1 × 2 MMI for splitting the input light into two and the other 2 × 2 MMI for combining two light signals that have experienced the different amount of phase shift. In the figure, two on-chip heater are shown that are used for controlling the length difference between two MZI arms. The bias controller should provide the correct voltage signal to one of these heaters so

Manuscript received 26 May 2023; revised 6 July 2023; accepted 16 July 2023. Date of publication 20 July 2023; date of current version 28 July 2023. This work was supported in part by the National Research Foundation of Korea (NRF) under Grant NRF2020R1A2C2015089 and in part by the Korea Institute of Science and Technology under Project 2E32422-23-024. *(Hyun-Kyu Kim and Kihun Kim contributed equally to this work.) (Corresponding author: Woo-Young Choi.)*

The authors are with the High-Speed Circuits and Systems Laboratory, Department of Electrical and Electronic Engineering, Yonsei University, Seoul 03722, South Korea (e-mail: yonsei142026@yonsei.ac.kr; khkim511@yonsei.ac.kr; alsguree@yonsei.ac.kr; yjji0314@yonsei.ac.kr; wchoi@yonsei.ac.kr).

Color versions of one or more figures in this letter are available at https://doi.org/10.1109/LPT.2023.3297177.

Digital Object Identifier 10.1109/LPT.2023.3297177

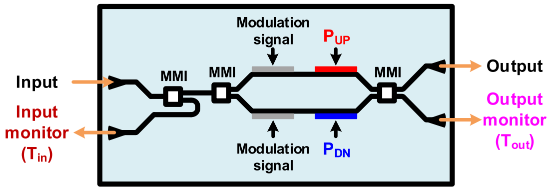

Fig. 1. Si-MZM Structure.

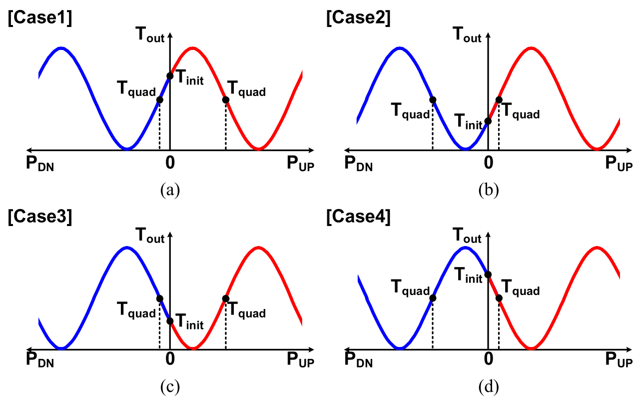

Fig. 2. (a), (b), (c), (d) Output power characteristics of MZM with 4 different initial conditions.

that the Si MZI is biased at the quadrature point. Although only one heater can be used for achieving the quadrature bias, having two heaters can reduce the heater power consumption by selecting the one which achieves the quadrature bias with less power consumption.

A. Scan Mode

Figure 2 shows four different cases of how the MZM transmission output power (T_{out} in Figure 1) changes with P_{UP} (shown in red) or P_{DN} (shown in blue) depending on the initial uncertainty in the MZM arm length difference. In this figure, T_{quad} represents the quadrature point where the Si MZM is desired to be. T_{init} represents initial T_{out} when no heater voltage is applied. As can be seen in the figure, the power consumption can be reduced by selecting P_{DN} for cases shown in Figure 2(a) and 2(c), or P_{UP} for cases shown in Figure 2 (b) and 2(d).

The four cases shown in Figure 2 can be distinguished by the sign of slope at T_{init} and whether T_{init} is larger or smaller than T_{quad}. For a given Si MZM, our controller scans P_{UP}, makes decision on these two conditions, and determines which among four different cases the given Si MZM belongs to and which heater to use. The flow chart given in Figure 3 explains details of this decision process. Then, it applies P_{UP} or P_{DN} so that the Si MZM is biased at the quadrature condition. During the scan mode, the input optical power is assumed the same. Although the controller finds the quadrature bias point, this scheme can be used for finding any MZM transmission point with a simple modification of the control code.

B. Lock Mode

In order to maintain the Si MZM at the quadrature condition achieved in the scan mode against any ambient temperature

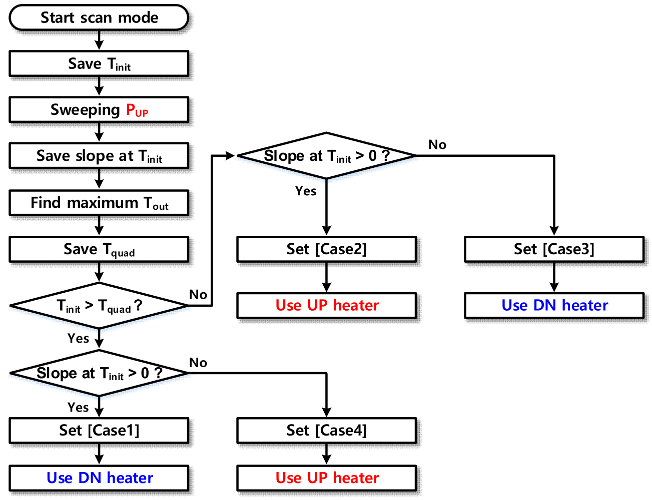

Fig. 3. Flowchart of the scan mode operation.

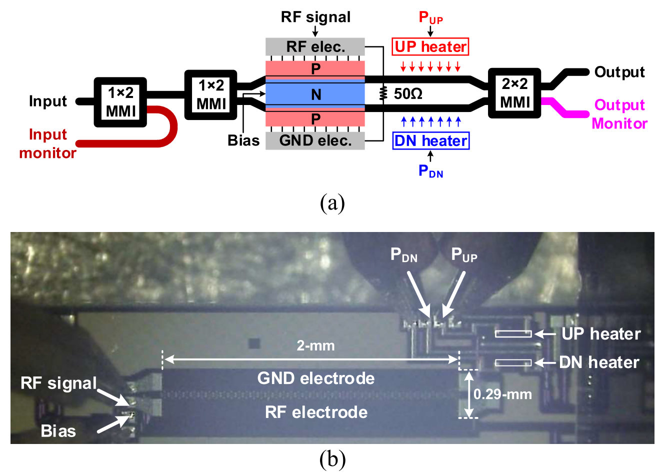

Fig. 4. (a) Block diagram of fabricated Si-MZM and (b) its chip microphotograph.

change, the dithering method [8] is used. The value of P_{UP} or P_{DN} determined in the scan mode is intentionally dithered while T_{out} is monitored. If it is found that T_{out} deviates from the desired value, P_{UP} or P_{DN} is changed so that the desired value can be maintained.

If there is any change in the input optical power, this dithering technique does not work properly. In order to prevent this, the input optical power is monitored with T_{in} shown in Fig. 1 and used for normalizing T_{out}.

III. Experimental Verification

In order to verify our Si MZM bias control scheme, a Si single-drive push-pull MZM (SPPMZM) [9] fabricated by a Si photonic foundry service is used. Figure 4(a) schematically shows the device structure and Figure 4(b) shows the chip microphotograph. The total insertion loss of our Si SPPMZM is 14-dB when it is bias at the quadrature point. This is due to 3-dB loss for the input power monitoring 1 × 2 MMI, 8-dB by the Si SPPMZM device itself at the quadrature point, and 3-dB for the output 2 × 2 MMI. The Si SPPMZM has 2-mm length PNP-doped junction with 500-nm wide rib waveguide.

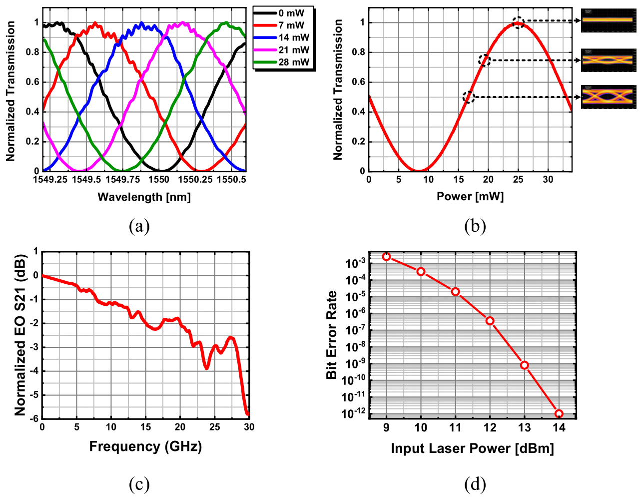

Fig. 5. (a) Measured transmission curve with driving UP heater. (b) Measured characteristic curve with driving UP heater and measured 25-Gb/s eye diagram at several heater power. (c) Measured EO frequency response of Si SPPMZM. (d) Measured BER performance of Si SPPMZM for 25-Gb/s PRBS-31 data.

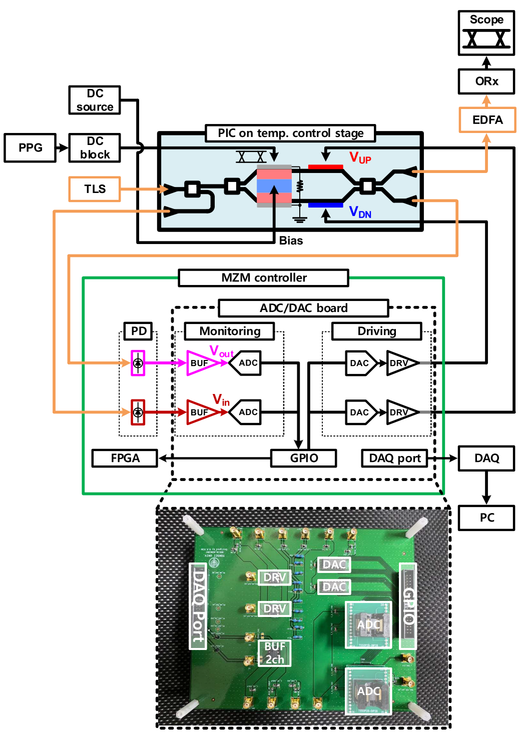

Fig. 6. Block diagram of measurement setup.

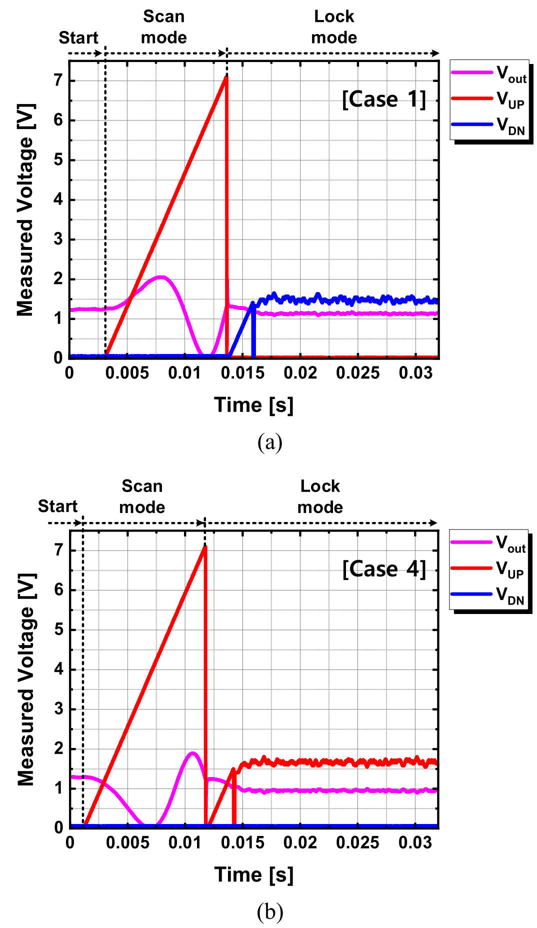

Fig. 7. Measurement result of the operation of scan mode at the laser wavelength of (a) 1549.5-nm and (b) 1550.5-nm.

The phase shifter efficiency is 3.75×10^{-5}/V. The device has built-in metal heaters as shown in Figure 4(a) and 4(b), that are used for the bias controller.

Figure 5(a) shows the measured transmission characteristics with different P_{UP} values. For this measurement, the device is placed on a stage whose temperature is maintained at 25 °C. Figure 5(b) shows how T_{out} changes with P_{UP} when the input wavelength is fixed at 1550.38-nm. Also shown are 25-Gb/s PRBS31 eye diagrams measured at different P_{UP} values. As can be seen, the eye quality greatly depends on P_{UP} and it is very important to find the optimal P_{UP} for any given MZM device. Fig. 5(c) shows the measured EO frequency response of the Si SPPMZM, whose 3-dB bandwidth is about 23-GHz. Fig. 5(d) shows the measured BER of the Si SPPMZM at the quadrature point for 25-Gb/s PRBS-31 data.

Figure 6 shows the block diagram of the MZM bias controller. For measurement, 12-dBm optical input is applied to the MZM using a C-band tunable laser source (TLS) through a grating coupler. The light signals coming out of the output port and the input monitor port of the MZM are delivered through grating couplers and fiber to photodetectors on the control board. One of MZM output is connected to the EDFA, optical receiver, and oscilloscope. The driving circuit output of the control board is connected to the built-in heaters in the MZM.

The ADC/DAC board consists of monitoring circuits and driving circuits on the FR4 PCB. The monitoring circuit includes two buffers that convert PD output into the voltage signal and two 25-MS/s ADCs. The I-V conversion gain of the buffer is 15-kV/A for output monitoring and 1.2-kV/A for input monitoring. The driving circuit consists of two 8-bit DACs and two drivers. The bias controller can drive the heater up to 33-mW, corresponding to $P_{2\pi}$ of the fabricated Si SPPMZM. The measurement data were provided to the data acquisition (DAQ) module. An FPGA performs the logic operation required for the control with 47-kHz clock signal. If the bias controller is implemented with an integrated circuit, a much higher clock frequency can be used.

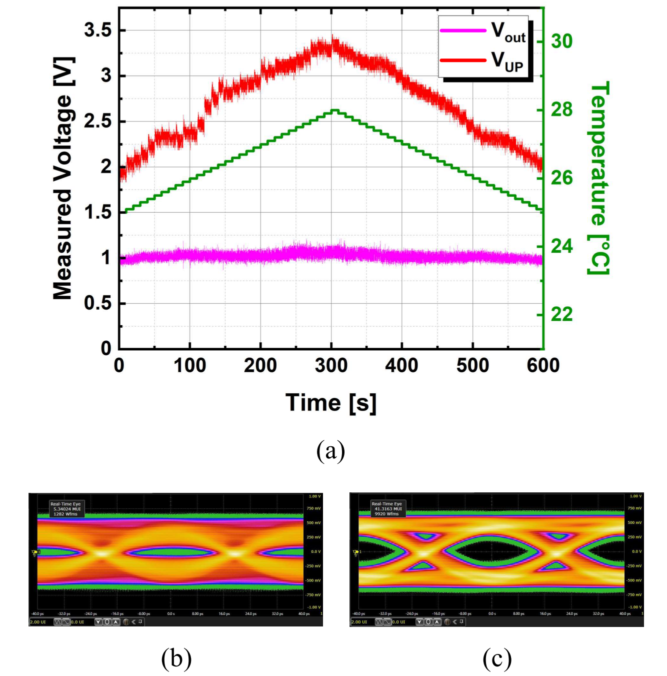

Fig. 8. (a) Measurement result when the stage temperature changes and (b) 25-Gbps eye diagram without controller and (c) with the controller.

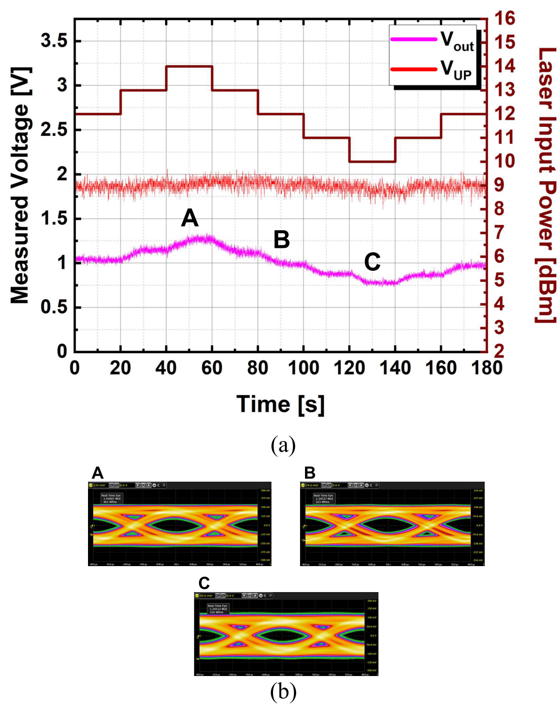

Fig. 9. (a) Measurement results when input optical power changes and (b) 25-Gbps eye diagrams at three sampling points.

Figure 7 (a) and (b) show the measured V_{out}, the buffered PD output, and the V_{UP}, V_{DN}, the voltages supplied to UP and DN heaters, respectively, when the MZM is controlled by the controller for two different cases. In the first case (Figure 7(a)), $\lambda = 1549.5$-nm is used for emulating Case 1 in Figure 2, and in the second case (Figure 7(b)) $\lambda = 1550.5$-nm is used for emulating Case 4 in Figure 2. It can be seen that in the first case (Figure 7(a)) the controller correctly selects DN heater and in the second case (Figure 7(a)) UP heater.

Figure 8(a) shows the measured V_{out} and V_{UP} for $\lambda = 1550.5$-nm when the stage temperature is intentionally raised from 25 °C to 28 °C and then lowered back to 25 °C, with 0.1 °C change every 10 seconds in the lock mode. Figure 8(b) and 8(c) show 25-Gb/s PRBS-31 eye diagrams measured during this change with and without the controller, respectively. These results demonstrate that the controller provides the proper heater voltages so that the eye quality can be maintained even when the environmental temperature changes.

Figure 9 shows the measured V_{out} and V_{UP} when the input optical power increases 2-dB from the initial value of 12-dBm, decreases 4-dB, and then increases 2-dB. The input optical power changes in steps since the TLS used does not allow continuous output power change in a reliable manner. Also shown are eye diagrams at three sampling points, which confirm that the optimal bias condition is maintained even if the input optical power changes.

IV. Conclusion

We successfully demonstrated a bias controller for the Si photonic single-drive push-pull MZM. The controller determines the heater providing less power consumption and achieves the quadrature bias condition in the scan mode and locks this condition against any ambient temperature or input optical power fluctuations. Our results should be of great help for realizing any Si PICs having Si MZMs that can achieve high performance with less power consumption.

Acknowledgment

The authors would like to thank IC Design Center (IDEC) for EDA tool support.

References

[1] L. Liao et al., "High speed silicon Mach–Zehnder modulator," *Opt. Exp.*, vol. 13, no. 8, pp. 3129–3135, Apr. 2005, doi: 10.1364/opex.13.003129.

[2] Y. Long, L. Zhou, and J. Wang, "Photonic-assisted microwave signal multiplication and modulation using a silicon Mach–Zehnder modulator," *Sci. Rep.*, vol. 6, no. 1, p. 20215, Feb. 2016, doi: 10.1038/srep20215.

[3] S. Liu et al., "Microwave pulse generation with a silicon dual-parallel modulator," *J. Lightw. Technol.*, vol. 38, no. 8, pp. 2134–2143, Apr. 15, 2020, doi: 10.1109/JLT.2020.2964102.

[4] X. Yuan, Y. Zhang, J. Zhang, and M. Zhang, "Any bias point control technique for Mach–Zehnder modulator," in *Proc. Asia Commun. Photon. Conf. (ACP)*, Nov. 2014, pp. 1–3, doi: 10.1364/acpc.2014.ath3a.37.

[5] Y. Fu, X. Zhang, B. Hraimel, T. Liu, and D. Shen, "Mach–Zehnder: A review of bias control techniques for Mach–Zehnder modulators in photonic analog links," *IEEE Microw. Mag.*, vol. 14, no. 7, pp. 102–107, Nov. 2013, doi: 10.1109/mmm.2013.2280332.

[6] M.-H. Kim, B.-M. Yu, and W.-Y. Choi, "A Mach–Zehnder modulator bias controller based on OMA and average power monitoring," *IEEE Photon. Technol. Lett.*, vol. 29, no. 23, pp. 2043–2046, Dec. 1, 2017, doi: 10.1109/lpt.2017.2762331.

[7] X. Zhu, Z. Zheng, C. Zhang, L. Zhu, Z. Tao, and Z. Chen, "Coherent detection-based automatic bias control of Mach–Zehnder modulators for various modulation formats," *J. Lightw. Technol.*, vol. 32, no. 14, pp. 2502–2509, Jul. 1, 2014, doi: 10.1109/JLT.2014.2328997.

[8] H.-K. Kim et al., "Si photonic-electronic monolithically integrated optical receiver with a built-in temperature-controlled wavelength filter," *Opt. Exp.*, vol. 29, no. 6, pp. 9565–9573, Mar. 2021, doi: 10.1364/oe.418222.

[9] P. Dong, L. Chen, and Y.-K. Chen, "High-speed low-voltage single-drive push-pull silicon Mach–Zehnder modulators," *Opt. Exp.*, vol. 20, no. 6, pp. 6163–6169, 2012, doi: 10.1364/oe.20.006163.